Targeted Autonomous Indoor Flight of a Rotary-Wing MAV

Svetlana Potyagaylo
PhD Student
Faculty of Aerospace Engineering
svetap@tx.technion.ac.il

Omri Rand
Professor
Faculty of Aerospace Engineering
omri@aerodyne.technion.ac.il

Yaron Kanza
Associated Professor
Faculty of Computer Science
kanza@cs.technion.ac.il

Technion, Israel Institute of Technology
Haifa, 32000, Israel

ABSTRACT

The paper is focused on the development of algorithms for Autonomous Rotary-Wing Micro Aerial Vehicles (RW MAVs) in indoor GPS-denied environments. In such missions, GPS may be unavailable and the map of the environment is a priory unknown. This paper presents a modular system consisted of the required components for flying RW MAVs in indoor environments. These components include the methods for MAV's position estimation, planning a flight path toward a target location while taking into account detected obstacles and maneuverability limitations of the vehicle, and for calculating flight commands to fly along the planed path. The methodology is based on a lightweight laser range finder as a sole onboard sensor. Moreover, only one of the system components requires knowledge about the MAV's dynamic model. The simulation results illustrate the effectiveness of the system modules.

INTRODUCTION

In recent years, MAVs received a special attention because of their usefulness in various military and civil applications and the significant advances in onboard computational capabilities. The small size and maneuverability of MAVs make them widely spread for indoor scenarios. These scenarios create new challenges since the operation methodology cannot rely on GPS signals for identifying their location, due to poor reception, or no reception at all, of the signal. Compared with fixed-wing vehicle that must maintain a minimum speed, RW MAVs are commonly used platforms for indoor tasks due to their hovering ability.

In this paper we study the problem consisted in autonomous navigation of RW MAV from initial known position and orientation to a definite final goal, while the map of the environment is a priori unknown. In order to safely complete the mission, the vehicle faces different tasks during the flight. The MAV operating in GPS-denied environments has to be able to identify its position (e.g. two coordinates and heading angle in 2D case) merely based on its surrounding. Because the map is a priori unknown, the vehicle need to sense the environment and construct the map simultaneously based on some estimation of its position. This task is widely known as Simultaneous Localization and Mapping (SLAM) (Ref. 1). Once the vehicle identifies its location, it can move towards the goal. Thus, the next task is determination of paths that are collision-free with the obstacles detected so far. In addition, the MAV should compute the control commands necessary for flying along a desired trajectory, while taking into account the limitations such as ability to accelerate or slow down, the ability to turn at its current speed, etc. The existence of system errors, disturbances, uncertainty and changes in the environment during the flight lead to additional complications in the required algorithms and their coupling.

A great progress has been made in each of the above listed tasks for navigation of ground robots and fixed-wing aerial platforms. However, the implementation of most of the existing algorithms is not so straightforward to RW MAVs. First, RW MAVs have a considerably limited payload capability, so the use of heavy sensors or a set of lightweight sensors is usually infeasible. Second, the dynamics of flying vehicles, and especially of RW vehicles, is more complex and faster than that of ground robots and contains many restrictions and constraints. This makes the MAVs problematic to control and model. Finally, navigation commands must be provided instantly, whereas onboard computing time is very limited. Although RW MAVs can interrupt the flight and hover (i.e. momentarily stop to allow onboard calculation to be completed), this is not desired because it decreases endurance and increases vehicle's vulnerability.

Thus, for an autonomous flight of a RW MAV in a GPS-

Presented at the American Helicopter Society 68th Annual Forum, Fort Worth, Texas, May 1-3, 2012.

denied environment, the following ingredients are essential:

- A method for estimating the position of the vehicle: In this paper, the position of the MAV is calculated in the *Position Estimation (SLAM) module* based on the *model-free SLAM method* that allows to estimate the location of the MAV simultaneously with updating the map of the environment.
- A method for path planning: In this study we developed the *Path Planner module* that employs two methods for path planning – an *A* graph search* for global planning and a *potential field method* (PFM) for local path calculating.
- A method for computing control commands: The proposed system includes the *Controller module* that calculates the navigation commands to move the MAV along the planned path.

Several papers studied autonomous navigation of RW MAVs in GPS-denied environments. For example, Shen et al. (Ref. 2) propose a quadrotor platform for autonomous multi-floor navigation in buildings using several sensors. The SLAM, the path planning and the control planning tasks are carried out onboard and in real time, so the system is described as “fully autonomous”. Similarly, Grzonka et al. (Ref. 3) used a quadrotor system but with laser range finder only. The quadrotor relies on an existing map to estimate its position and includes a laser mirror to deflect some of the laser beams in order to control the altitude. User interaction is allowed to control the vehicle flight altitude and heading and prevent collision with obstacles. He et al. (Ref. 4) used a quadrotor platform as well but focus was put on the motion planning algorithm. During the flight, the vehicle uses the existing map and laser range data to localize itself within the map. The algorithm ignores vehicle dynamics and tries to find a sequence of vehicle’s poses (position and orientation) required to move the vehicle from an initial state position to a goal position.

In contrast to the above approaches, our methodology addresses the problem of indoor navigation of a conventional helicopter MAVs (i.e. having a main-rotor tail-rotor scheme). The position estimation and mapping merely rely on laser scan data. The only onboard sensor is a lightweight laser range finder. Our approach takes into account the helicopter dynamics and limitations, however, it is model-free in the sense that it does not require estimating the position of the vehicle based on its dynamic model.

SYSTEM AND METHODOLOGY

We present now an overview of our methodology and of the modular system that executes it. A schematic diagram of the system and of its components is depicted in Fig. 1. The system includes a “position estimation module” (SLAM), a “path planner module” and a “controller module”. The architecture is modular so that each component can be used independently of the others.

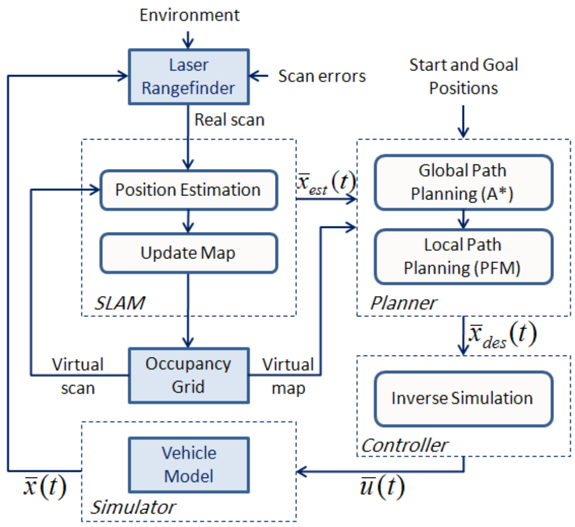

Fig. 1. The components of the system.

For localization and mapping, the system employs a *model-free SLAM* module (Ref. 5), which, differently from other SLAM modules, uses only one source of data (laser range finder) and does not use the dynamic model of the vehicle. Since the map of the environment is a priory unknown, detected obstacles are represented and stored in memory in the form of an *occupancy grid* (OG) (Ref. 6). The OG is used for performing a “virtual scan” as part of the SLAM. The virtual map is updated after each laser scan, when the position estimation is complete. The path planning module combines two algorithms – an *A* search algorithm* and a *potential field method* (PFM) (Ref. 7). The A* algorithm finds the shortest collision-free path from the current (estimated) position of the MAV toward the target position. This path provides waypoints that serve as intermediate goals for the PFM. We then apply the PFM to calculate a feasible path from the current position to the farthest waypoint which is within a line of sight from the MAV. This separation of the path planning task into two sequential algorithms is required due to the shortcoming of both global (A*) and local (PFM) planners as will be describe later on in Subsection . To determine control commands that fly the MAV along the planned trajectory, a module that uses an *inverse simulation* (IS) (Ref. 8) technique was developed. The module receives the desired flight vector and interprets it to control commands that are suitable for a RW MAV.

Fig. 2 presents schematically the steps of computing a flight path according to our methodology. It depicts the planned flight path, the actual flight path and the computed flight steps, and illustrates the process of computing the flight path. Initially, the MAV is located at a start position (x_0, y_0, ψ_0) with known coordinates. A laser scan provides initial data about the obstacles ahead. The scan results are

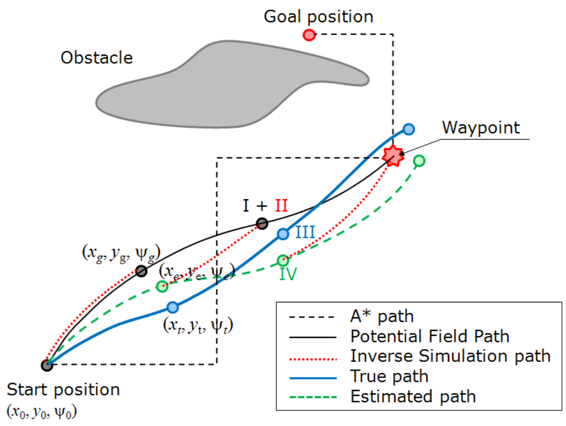

Fig. 2. The planned flight path (A* and PFM), the computed steps to fly along the planned path (IS), the estimated path (SLAM) and the actual (true) flight path.

added to the OG. Then, A* and PFM are employed consecutively to calculate the nearest waypoint and the next point (x_g, y_g, ψ_g) to arrive at (Stage I). The IS algorithm computes the control commands for arriving at this point (Stage II). This point serves as a guess for the position estimation process. After that, the control commands are executed (Stage III). The result of this stage is a point (x_t, y_t, ψ_t) that differs from the guess point due to errors in the commands and in the execution, and due to unconsidered effects of the environment. The position estimation module matches two scans – a virtual scan in the virtual map when assuming that the MAV is located at the guessed point, and a real laser scan. The matching provides an estimation of the vehicle position (x_e, y_e, ψ_e) (Stage IV). Simultaneously, the map updating process is proceeded.

Before the next iteration, the validity of the planned paths of A* algorithm and PFM are checked. In the case of collision with newly detected obstacles or possibility to move the waypoint forward along the A* trajectory, the A* or PFM paths are recalculated. On the next iteration, all the stages are repeated, until arriving at the goal.

The system uses two main coordinate frames – a *global coordinate system* and a *body coordinate system*. The origin of the global coordinate system is arbitrarily fixed and its axes x_gl and y_gl are oriented to the east and to the north, respectively. Navigation of the MAV is carried out within this frame. The body coordinate system is related to the MAV itself – the origin is located at the center of gravity (CG) of the MAV, the x_b-axis points forward and the y_b-axis is to the left side of the MAV. Computing control commands using these coordinate systems is presented in Subsection .

THE MAIN MODULES

Localization and Mapping

SLAM is considered as one of the most fundamental problems in robotics dealing with the necessity of building a map of an unknown environment along with estimation of robot position within this map. This problem arises since a model or map of the environment is a priori unavailable and the robot movements are not perfect and deterministic. SLAM is often referred to be a “chicken-and-egg” problem (Ref. 9): an environment map is assumed to be available for solving a localization problem while an accurate pose estimate is needed to build a map. These two problems can be solved apart relatively easily assuming the presence of an environment map for the localization problem and the awareness of the vehicle’s pose for the second problem independently. But the absence of both the map and the information of the vehicle pose leads to necessity of solving these problem simultaneously.

Traditionally, SLAM algorithms solve the problem using Extended Kalman filters (Ref. 1) or Particle Filters (Ref. 10). These methods use a probabilistic model to represent the observations, and a dynamic model of the vehicle. The Model-Free SLAM algorithm that we propose here does not rely on any particular vehicle model.

Our algorithm uses an occupancy grid in which each cell represents a sub-area and contains the number of laser “hits” registered for that sub-area. The OG is also used for performing a *virtual scan* produced by a series of ray casting operations, searching for occupied cells. The virtual scan is executed with respect to guessed position and heading of the vehicle. It is then compared with a laser scan obtained from the actual laser range finder of the MAV. The difference between the *virtual* and *real* scans is the basis for the position estimation. We refer to it as *scan matching* (Ref. 11).

We employ Algorithm 1 for computing the position estimation of the MAV, using the scan matching method. In each iteration, the algorithm “guesses” the shift between the actual location of the vehicle and the guess position and compares the computed virtual scan to the roto-translated actual scan in the real world. Using a adaptive direct search (Ref. 5), a new shift is computed. The process terminates when a location that minimizes the error between the actual scan and the virtual scan is discovered, and this location is returned as the estimated location of the vehicle.

While the search estimates the position of the MAV, the map updating process can be proceeded. However, map updating is performed only if the matching succeeds, i.e. the result of the scan matching is below a defined threshold. This is required since the OG serves as an average of all previous laser scans and thus, if the virtual scan is not accurate enough, the updating of the OG will not be accurate as well, which would lead to a rapidly growing of the error in the MAV’s position estimation.

The position estimation provided by the SLAM module is used for velocity estimation as well. The velocities in the x and y directions are updated based on the displacements in these directions between the previous and current posi-

Algorithm 1 Estimate a position of the MAV, using Scan Matching

```
Consider an initial guess location and heading of the MAV: $x = x_g, y = y_g$ and $\psi = \psi_g$, which will be denoted by the vector $(x_g, y_g, \psi_g)$.
Scan the environment using a laser range finder with respect to the actual (true) position of the MAV $(x_t, y_t, \psi_t)$, and store the resulting data as a vector $(r_r, \theta_r)$, for the scanned angles in the range $-\theta_{max} \leq \theta \leq \theta_{max}$.
Create a new virtual scan $(r_v, \theta_v)$, based on the OG and the initial guess $(x_g, y_g, \psi_g)$.
Consider the initial shift in the position and heading between the guess position $(x_g, y_g, \psi_g)$ and the true position $(x_t, y_t, \psi_t)$ as: $(\Delta x_g, \Delta y_g, \Delta \psi_g)$.
repeat
    Convert the real laser data $(r_r, \theta_r)$ so that it would look as if it was measured from the guess position using the initial guess shift. At this step the following equations are used:
        $x' = r_r \cdot \cos(\theta_r + \Delta\psi_g) + \Delta x_g;$
        $y' = r_r \cdot \sin(\theta_r + \Delta\psi_g) + \Delta y_g;$
        $r' = \sqrt{x'^2 + y'^2};$
        $\theta' = \tan^{-1}\left(y'/x'\right).$
    The result of this step is roto-translated real scan $(r', \theta')$.
    Applied series of filters to the roto-translated real scan $(r', \theta')$ in order to leave only valid points.
    Calculate a norm of the error that represents the discrepancy between $(r', \theta')$ and $(r_v, \theta_v)$, only for the range covered by both.
    Use a *adaptive direct search* for computing a new guess vector $(\Delta x_g, \Delta y_g, \Delta \psi_g)$.
until The guess vector minimizes the error norm.
return $(\Delta x_g, \Delta y_g, \Delta \psi_g)$
```

tion estimations. The shift in the heading angle is used for updating the MAV velocities in the body coordinate system.

Path Planning

Navigating a MAV to a target location is not a simple task. First, obstacles are only discovered during the flight, so the path should be constantly updated. Secondly, the flight trajectory should be as short as possible. Thirdly, the path should comply with maneuverability limitations of the MAV, e.g. changes in the flight orientation should not be acute. The path planning module combines A* search method and a PFM to navigation of RW MAVs. The A* search algorithm is used for planning an initial global path that provides the waypoints. Then in each iteration, the PFM takes the farthest waypoint in line of sight (with respect to the location of the MAV) on the path computed by A*, as an intermediate goal, and it returns a feasible trajectory to that goal, as a reference for the computation of the control commands.

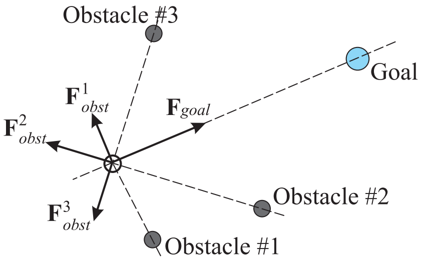

Fig. 3. The Potential Field Method illustration.

A* is a general search algorithm that traverses a graph of nodes (or grid cells) by following the lowest cost associated with each node. The cost of the node is calculated base on a heuristic function, that estimates the path cost from the current node to a goal. This process continues until the goal is reached. In this work, the Euclidean distance from the current MAV position to the target was chosen as one of the widely used heuristic functions for such tasks.

A* is applied over an OG that has the same structure as the grid of SLAM but uses larger cells to overcome the drawback of A* algorithm of its memory requirement. A* computes a path to the target, allowing eight directions of movement, including moving on the diagonals of cells. It produces trajectories that consist of straight segments with sharp turns in the vertices, that makes such path to be irreconcilable with the MAV dynamics. Clearly, a helicopter can cope with such changes by frequent "stop and re-orient" procedures; however, this type of maneuvering is undesired. The PFM is serve to cope with this problem. It takes into account the kinematic constraints of the MAV (mainly minimum turning radius) and smooths the path, making it viable.

The PFM considers the MAV as a particle moving in a force field produced by the repulsive and attractive forces from obstacles and goal, respectively. The idea of having obstacles that "induce" forces over a vehicle has been first suggested by Khatib (Ref. 7) with respect to manipulators. The resultant force acting on a vehicle at any position in the force field can be expressed as the sum of repulsive forces from obstacles and the attractive force towards the goal (see Fig. 3):

$$\vec{F}_{rez} = \vec{F}_{goal} + \sum_{i=1}^{N} \vec{F}^{i}_{obst}, \tag{1}$$

where N is the number of obstacles; $\vec{F}^{i}_{obst}$, $i = 1 \ldots N$ are the repulsive forces; $\vec{F}_{goal}$ is the attractive force towards the goal and $\vec{F}_{rez}$ is the resultant force.

In this paper, the attractive force of the goal and the repulsive forces of the obstacles are defined as:

$$\overline{F}_{goal} = I_{goal}\frac{\overline{x}_{goal}-\overline{x}_{MAV}}{d_{goal}};$$
$$\overline{F}_i = I_{obst}H_i\frac{\overline{x}_i-\overline{x}_{MAV}}{d_i}, \tag{2}$$

where I_{goal} is the constant positive intensity level of the goal, $\overline{x}_{goal} = \left(x_{goal}, y_{goal}\right)$ is the goal position, $\overline{x}_{MAV} = \left(x_{MAV}, y_{MAV}\right)$ is the current (estimated) MAV position, d_{goal} is the distance from the current MAV position to the goal position. Similarly, I_{obst} is the negative intensity level of the obstacle, inversely proportional to the distance d_i from the cell center to the center of mass of the vehicle, H_i is the hit count of the cell (see Subsection), and $\overline{x}_i$ is the cell center.

Yet, overlaying attractive and repulsive potential functions as described above can result in a local minima where the resulting force is equal to zero at a position other than the target. A typical scenario for this case is when the vehicle faces an obstacle and the target is behind the obstacle. This is the major drawback of the potential field approach. Thus, the main issue is escaping from the local minima. The waypoint achieved by the A* serves as a temporary goal that is always in line of sight and it precludes such cases.

The intensities of the goal and of the obstacles and the mass of the particle are "virtual" in the sense that they are used only for trajectory planning – they are chosen in a way that ensures the kinematic constraints (mainly the turning radius of the MAV).

Inverse Simulation

Given a trajectory to the target, it is required to compute control commands to fly along it. Several general methods for motion planning and for computing a sequence of control commands are based on optimal control tools (Ref. 12) and dynamic programming (Ref. 13). Some techniques of path planning can be extended for motion planning as well, for example, the rapidly-exploring random tree algorithm (Ref. 14) and genetic algorithms (Ref. 15). These approaches are unsuitable for helicopters whose maneuverability capabilities are described using complex and highly nonlinear models. Thus, an alternative approach, namely *inverse simulation*, has been developed. While simulation is traditionally used for solving the vehicle equations of motion to find the system response to a prescribed sequence of control commands, inverse simulation reverses this process and determines the controls required to produce a given response, defined in terms of the system variables or states.

Inverse simulation is commonly divided into two distinct approaches: a *differentiation-based* approach (Ref. 16) and an *integration-based* approach (Ref. 17). The controller module of the system, we present here, uses the integration-based approach. This approach is based on repeated numerical integration of the motion equations of the helicopter. An important advantage of the integration-based method is not being model-specific. This means that it can be used for different models without changing the algorithm. One of the drawbacks of this approach is that it is considerably slower than the differentiation-based method.

In the general case, the mathematical model of the vehicle may be written as the following system of the first-order differential equations:

$$\dot{\overline{s}} = \overline{f}\left(\overline{s}, \overline{u}\right), \tag{3}$$

along with the initial conditions $\overline{s}_0$. In the above equation, $\overline{s}$ is the system state vector, $\overline{u}$ is the control vector, and $\overline{f}$ is a nonlinear function that represents the applied forces and moments, typically referred to the CG and originated from different sources such as aerodynamic, structural, gravitational and inertial sources, and from different subsystems of a helicopter.

We use a model of the helicopter with six degrees of freedom, in addition to the fuselage attitude (Euler) angles and the main rotor flapping angles:

$$\overline{s} = \left(u, v, w, p, q, r, \psi, \theta, \phi, \beta_0, \beta_{1c}, \beta_{1s}\right)^T, \tag{4}$$

where u, v, w are the translational velocity components; p, q, r are the rotational velocity components; ψ, θ, ϕ are the body yaw (heading), pitch and roll attitude angles, and $\beta_0, \beta_{1c}, \beta_{1s}$ are the main rotor flapping angles. These components are given with respect to the body frame.

Having defined the model, we proceed to the inverse problem which looks for the controls required for flying the helicopter in a specific trajectory and a given speed. For that purpose, the helicopter motion equation is supplemented by an additional output equation that associates the state vector with the required quantities:

$$\overline{h} = \overline{g}\left(\overline{s}, \overline{u}\right); \tag{5}$$

where $\overline{h}$ is the output vector, $\overline{g}$ is a nonlinear function.

In this paper, the integration-based inverse simulation method initially guesses the control inputs $\overline{u}$, integrates the vehicle motion equations, to achieve the desired output vector at the next iteration. The difference between the actual flight vector and the desired flight vector is then used to calculate the estimation of the control inputs for the next path computation step. The equations of motion at the k-th time step can be written as:

$$\overline{s}\left(t_{k+1}\right) = \overline{s}\left(t_k\right) + \int_{t_k}^{t_{k+1}} \overline{f}\left(\overline{s}\left(t_k\right), \overline{u}^m\left(t_k\right)\right)dt;$$
$$\overline{h}\left(t_{k+1}\right) = \overline{g}\left(\overline{s}\left(t_{k+1}\right), \overline{u}^m\left(t_k\right)\right), \tag{6}$$

where $\overline{u}^m\left(t_k\right)$ is the m-th estimation of the control inputs. The next iteration of the control input is estimated using the residual function which represents the difference between the desired output vector and the actual one and must eventually vanish.

For simplicity and for allowing onboard implementation within the limitations of current technology, a linearized mathematical model of the helicopter, about a trim state was developed. The assumed linear model can be expressed in the following form:

$$\begin{aligned} \delta\dot{\bar{s}} &= \mathbf{A}\delta\bar{s} + \mathbf{B}\delta\bar{u}; \\ \bar{h} &= \mathbf{C}\bar{s}, \end{aligned} \tag{7}$$

where $\delta\dot{\bar{s}}$ is the deviation of the state vector from its trim condition; $\delta\bar{u}$ is the deviation of the control vector from its trim-state vector; **A**, **B** and **C** are constant state, control, and transformation matrices.

The state, control and output vectors are:

$$\begin{aligned} \bar{s} &= (u, v, w, p, q, r, \psi, \theta, \phi)^T; \\ \bar{h} &= (\dot{x}_e, \dot{y}_e, \dot{z}_e, \psi)^T; \\ \bar{u} &= (\theta_0, \theta_{1c}, \theta_{1s}, \theta_{tr})^T, \end{aligned} \tag{8}$$

where $\dot{x}_e$, $\dot{y}_e$, $\dot{z}_e$ are the velocity components of the vehicle in the global coordinate system; θ_0 is main rotor collective pitch angle; θ_{1c}, θ_{1s} are the main rotor lateral and longitudinal cyclic pitch angles; θ_{tr} is the tail rotor collective pitch angle. In this work we assumed that the MAV is equipped with a stabilization system that provides the required balance about roll, pitch and heading directions, to overcome the high sensibility of MAVs to external disturbances such as wind gusts, due their light weight and small size.

It should be noted that controller module performance and accuracy highly depend on the selection of the $\bar{s}$, $\bar{u}$ and $\bar{h}$ vector components. In this model, the inverse simulation is programmed to reach a certain velocity components $\dot{x}_e, \dot{y}_e, \dot{z}_e$ at the end of each step. It allows to omit the additional integration stage compared to the version of the output vector $\bar{h}$ with only coordinate components.

The above system and control matrices **A** and **B** consist of the partial derivatives of the nonlinear functions describing the helicopter motion and represent the changes in the forces and moments at the trim point due to the changes in the state vector (Ref. 18). These matrices were calculated using a detailed nonlinear simulation process for the nonlinear model of Equation (3), in which for given flight condition the trim state parameters were calculated. Then, a numerical differentiation of the derivatives of the state vector components $\left(\dot{u}, \dot{v}, \ldots, \dot{\phi}\right)$ with respect to the state vector components and the controls $\theta_0, \theta_{1c}, \theta_{1s}, \theta_{tr}$ was carried out. The matrix **C** is a transformation matrix that interprets the velocity components u, v, w from the body coordinate system to the velocity components $\dot{x}_e, \dot{y}_e, \dot{z}_e$ in the global earth coordinate system:

The inverse simulation module was tested to evaluate the performance of unmanned helicopter model constructed earlier. For these purposes several mission-task-elements (MTEs) were selected and adopted based on the performance specification ADS-33D-PRF (Ref. 19). This specification was originally designed for full-sized helicopters used in military missions but the careful selection and proper adjustment of the performance parameters allow to use the specification for MAVs as well. In this paper, the following MTEs were picked out:

1. *Slalom*: The maneuver starts from the trim level flight and represents two smooth turns up to predefined lateral shift from the centerline to the both sides as shown on Fig. 4(a). The forward speed remains constant, and the coordinated level flight is assumed during the maneuver. After the maneuver ends up, the helicopter returns to the forward straight flight.

2. *Pirouette*: The maneuver is initiated at a hover over a point on the circumference of a circle with a given radius with the nose of the helicopter pointed to the center of the circle. The helicopter has to accomplish a lateral translation around the circle, keeping the nose pointed to the center of the circle as depicted on Fig. 4(b). The lateral speed after the acceleration phase maintains constant. The maneuver is terminated by the deceleration phase up to the stable hover.

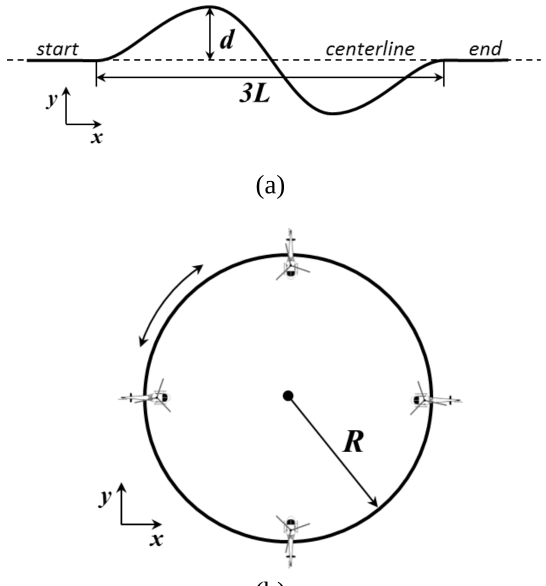

(a)

(b)

Fig. 4. Illustration of the maneuvers: (a) slalom; (b) pirouette.

For each maneuver the appropriate flight trajectory and required input for the inverse simulation algorithm were constructed. In what follows the predefined parameters and desired input are described for each maneuver.

1. *Slalom*: The input parameters for this maneuver are the trim forward speed $V[m/sec]$, the lateral displacement

$d[m]$ and the length of the maneuver flight path along the centerline $L[m]$ (see Fig. 4(a)). The total time of the maneuver is defined according to the defined trim speed V. The equations for coordinates and velocities in the x_e and y_e directions are:

$$\begin{aligned}
&x_e(t) = Vt\\
&y_e(t) = \frac{d}{8}\left(-81\xi(t)^3 + 135\xi(t)^4 - 81\xi(t)^5 + \right.\\
&\qquad\qquad \left. 21\xi(t)^6 + 2\xi(t)^7\right)\\
&\dot{x}_e(t) = V,\\
&\eta(t) = \frac{\partial y_g}{\partial \xi} = \frac{d}{8}\left(-243\xi(t)^2 + 540\xi(t)^3 - \right.\\
&\qquad\qquad \left. 405\xi(t)^4 + 126\xi(t)^5 + 14\xi(t)^6\right),\\
&\dot{y}_e(t) = \frac{V}{L}\eta(t),\\
&\psi(t) = tan^{-1}\left(\frac{1}{L}\eta(t)\right),
\end{aligned} \tag{9}$$

where $\xi(t) = Vt/L$.

2. *Pirouette*: The input parameters are the time of acceleration/deceleration phase $t_{trans}[sec]$, the lateral constant speed $V[m/sec]$, the radius of the turn $R[m]$ and the direction of the turn γ ($+1$ in clockwise case or -1 in counter-clockwise case). The total time of the maneuver is defined according to the defined trim speed V. The maneuver is performed by changing the lateral velocity of the helicopter smoothly from zero state to the defined value V, maintaining it constant during one revolution and that decreasing it smoothly to the zero value. The smooth change of the lateral velocity during acceleration and deceleration phases is supplied by the following polynomial functions:

   acceleration phase:

   $$\dot{y}_e = V\left(35\xi(t)^4 - 84\xi(t)^5 + 70\xi(t)^6 - 20\xi(t)^7\right),$$

   deceleration phase:

   $$\dot{y}_e = V\left(1 - 35\xi(t)^4 - 84\xi(t)^5 + 70\xi(t)^6 - 20\xi(t)^7\right), \tag{10}$$

   where $\xi(t) = t/t_{trans}$.

   The equations for circle flight with constant lateral velocity are:

   $$\begin{aligned}
   &\psi(t) = -\gamma\frac{2\pi R}{V}t,\\
   &x_e(t) = R - R\cos(\psi(t)),\\
   &y_e(t) = \gamma R\sin(\psi(t)),\\
   &\dot{x}_e(t) = V\sin(\psi(t)),\\
   &\dot{y}_e(t) = V\cos(\psi(t)).
   \end{aligned} \tag{11}$$

For all maneuvers it was assumed that the parameters of the desired vector that remain unchangeable during the maneuver are equal to zero. Additionally, the short phases of the trim forward flight or stabilized hover were embeded before and after each maneuver. The simulation results of the maneuvers in terms of desired and obtained flight trajectory, control commands and attitude angles are shown on Fig. 5 and on Fig. 6.

As seen on Fig. 5(a), the trajectory obtained by the direct simulation of the helicopter model with the control commands calculated by the Controller module coincides with the desired trajectory for slalom maneuvers. The slight deviation in the z direction can be observed due to the presence of the trim vertical velocity. The attitude angles for the slalom maneuver shown on Fig. 5(c) indicate that the maneuver is carried out by changing mostly the roll angle ϕ with amplitude 1° around its trim value. The amplitude of the pitch angle is twice smaller. The changes in the control commands for the slalom are shown on Fig. 5(b), where the tail rotor collective pitch command provides the desired variations in heading. The obtained trajectory for pirouette maneuver as depicted on Fig. 6(a) also matches the desired trajectory with high accuracy. The attitude angles and control commands remain constant the during circle flight with contact lateral speed that is correlated with the theory. The acceleration and deceleration for this manurer are provided by the cyclic main rotor control and, consequently, by the changes in both pitch and roll angles.

SIMULATION RESULTS

To examine the effectiveness of the proposed system and of its components, we conducted simulations and tested the components separately and combined. We consider the simulation as a powerful tool and an important stage in the system development process. It gives a rich variety of the possible means for investigating the system, estimating its performance and checking the collaborative work of its modules in different regimes and scales. The task considered in this paper belongs to the class of the problems for which the simulation is highly effective. The numerous unrealistic environments may be constructed and verified; the operating regimes and scales may be selected such that are unobtained in real experiments. Moreover, the simulation allows to measure the accuracy of the system with very high precision, that is almost impossible in real life, where the full information about the vehicle state and the environment properties are often unavailable.

Although we used specific parameters in our simulations, the parameters can be changed and the approach can be applied to navigation at different scales. Considering the length of the OG cell as a reference unit, we can replace it by a real unit, and change the other parameters proportionally.

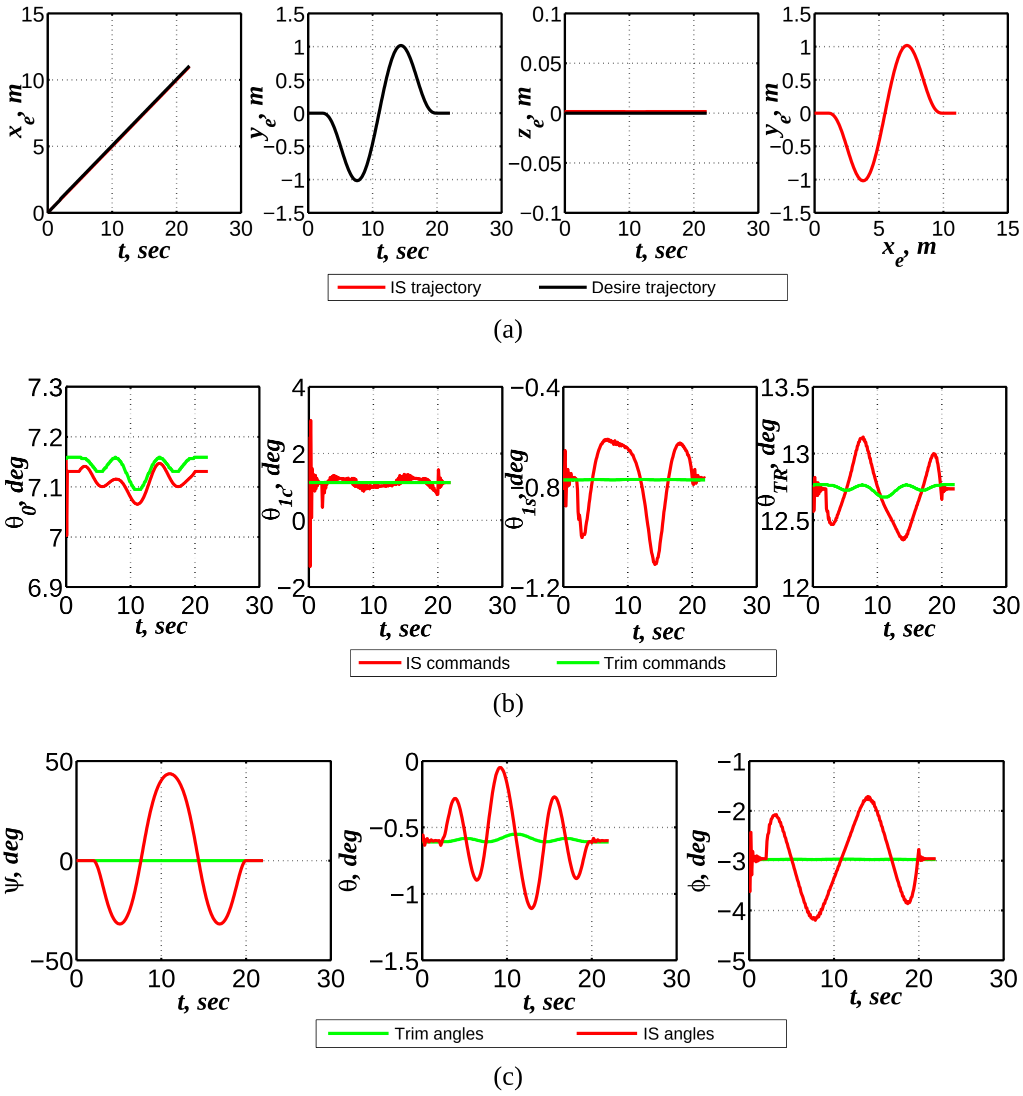

(a)

(b)

(c)

Fig. 5. The results of the Inverse Simulation for slalom maneuver: (a) the desired and obtained trajectory; (b) the control commands calculated by Controller module; (c) the MAV's attitude angles.

Simulation Setup

In the simulation we assumed the use of the following components. As a single laser range finder we consider the Hokuyo 2D laser scanner (Ref. 20). This scanner has a maximum range of approximately $30m$, field of view of $270°$ and an angular resolution of $0.25°$. According to the specifications, the distance accuracy of the laser range finder is below 1% of the measured distance, at the worst case. Thus, in all the simulations we present, the noise level of "real" scans is 1.5%. The helicopter we considered is SR RTF, manufactured by Blade, Horizon Hobby, Inc. (Ref. 21). It was chosen as a prototype for modeling the controller and simulator modules. The main parameters of the helicopter are: main rotor diameter of $552mm$, tail rotor diameter of $82mm$, weight of $340g$, length of $485mm$.

The actual model of the MAV includes the different sources of the uncertainness and noises such as wind gusts model and noises in the control commands. The wind model implies an injection of the wind velocity components normally distributed with zero mean and standard deviation of $0.2m/sec$ as a disturbance input to the vehicle respective channels. The command noise level is 2%.

The resolution of the OG was set so that cells have a size of $10 \times 10mm$. The cells of the A* OG are at size $500 \times 500mm$. The two constant parameters the PFM uses (the intensity of the goal force and fictitious mass of the vehicle) where chosen in a way that ensures the required smoothness of the flight trajectory. In addition, forces in PFM are computed only with respect to cells of the OG which are in the fore third of the field of view, i.e. $\pm 60°$ with respect to the heading vector. The algorithms are implemented in MATLAB combined with C++ mex-files, so

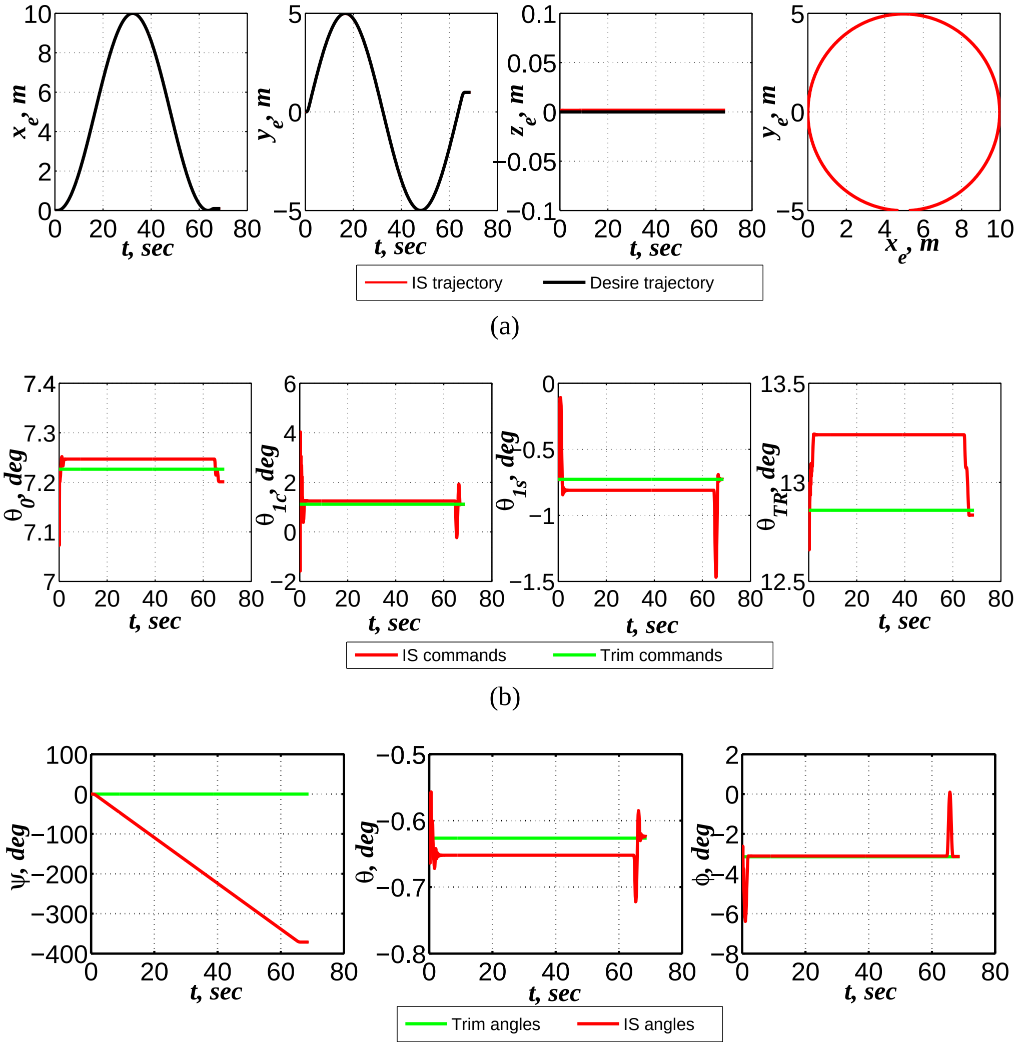

(a)

(b)

(c)

Fig. 6. The results of the Inverse Simulation for pirouette maneuver: (a) the desired and obtained trajectory; (b) the control commands calculated by Controller module; (c) the MAV's attitude angles.

the computational costs of the system modules were evaluated in terms of percentage of the total runtime.

The simulations were carried out in RAPiD/RaTE rotorcraft analysis software package (Ref. 22). It is designed to model and analyze general rotorcraft and rotary-wing based configurations. It is capable of modeling, analyzing and simulating general conventional helicopters (i.e. helicopters with a main and a tail rotor), tandem helicopters, coaxial and tiltrotor configurations. RAPiD/RaTE is also capable of analyzing propellers and various types of wind turbines. RAPiD/RaTE solution methodology is based on direct time domain integration and post-processed frequency analysis. RAPiD/RaTE has been review and display extensively (Ref. 23), (Ref. 24).

Results and Discussion

To demonstrate the effectiveness of our modular system, Fig. 7 illustrates the results of the SLAM, Path Planner and the Controller modules. In this figure, three successive snapshots of one of the simulated environments are depicted. Note that not all the obstacles are detected immediately due to the limitations of the laser range finder. Hence, the computed flight path must be adapted during the flight. The estimated A* and Potential Field paths are unremittingly checked for their validity according to the incoming data about newly detected obstacles. In the case of a collision between a planned path and a detected obstacle, the planned paths are recalculated.

The error plot demonstrates that the SLAM module provides highly accurate results for position estimation and heading angle and shows that no additional errors are accumulated through time. The true trajectory and estimated trajectory depicted in Fig. 7(a) also uphold the accuracy of the position estimation module. The control commands calculated in the controller module and the true controls that are passed to the simulator are shown on Fig. 7(b). The true commands are received from the control commands by adding a noise with Gaussian distribution with deviation of 0.5° and zero mean. The controller module does not take into account all the limitations of the control commands. Consequently, the commands can exceed their allowed margins. Therefore, a *limiter filter* adjusts the control to feasible values within the limits, before applying these commands in the simulator. The control commands are generated at frequency of $10Hz$ but the frequency of the SLAM and Path Planner modules is lower and is about $0.5-1Hz$.

In order to adjust the differences in the operation frequency of the different system modules, for each time step of the SLAM and Path Planner modules the polynomial function that allows the smooth modification of the velocity components and heading of the MAV from the current estimation to the desired values is created. The desired velocity and heading values are computed based on the position coordinates at the next time step provided by the Path Planner, and current flight regime of the vehicle. It was assumed that there are five flight regimes: (1) the normal flight with constant forward speed; (2) the transition regime from the forward flight to hover state; (3) hover; (4) the turn in hover; (5) flight resumption from hover. The current flight regime is selected relying on the information from all system modules. The nominal flight regime of the MAV is the forward flight with constant speed. The slight velocity deviations can be occurred during one time step due the guarantee to pass the required distance in $x-y$ plane for that step. The switching to another flight regime is conducted by the strong links between the modules.

For example, in the case, where the SLAM module failed to estimate the current position of the MAV at some point along the path, the algorithm autonomously cause the MAV to slow down and pass to a hover state. This hover regime may provide enough time for additional laser scans, their capturing and position estimation. This case is illustrated on the rightmost picture of Fig. 7(a). The another example of the collaborative work of the system modules is shown on the middle snapshot of Fig. 7(a), where the large changes in the heading are required. In this case, the algorithm also causes the MAV to hover at the point of changing the heading, to accomplish the turn in hover and then to resume the flight.

CONCLUSIONS

We presented a modular system for indoor navigation of RW MAVs toward a given target. The problem is studied for a vehicle that senses the environment using merely a laser rangefinder. The main challenges in such task are the following: (1) Position estimation – in the absence of a GPS signals, the location of the vehicle must be estimated according to the measurement of the environment. (2) Map updating – in the case of a priory unknown environment the map must be constructed based on the accurate information about the vehicle position. (3) Obstacle avoidance – the path planning should prevent collision of the MAV with obstacles. (4) Keeping the flight to be as short as possible – the planned path should not be much longer than what is necessary for completing the task. (5) Considering the dynamics of the vehicle – the control command for flying along the planned path should be in accordance with the flight abilities of the helicopter.

The proposed system consists of independent modules for position estimation, path planning, and computation of control commands. Our simulation results showed that:

1. Accurate location estimation is a crucial, yet difficult, task for navigating a MAV in a GPS-denied environment. Our results showed that the SLAM module is accurate without relying on any particular knowledge about model of the vehicle.

2. The absence of an a priori known information, about the environment and about the obstacles in it, prevents the usage of the majority of the existing path planning algorithms and reduces the effectiveness of others. The path planning module proposed in this study provides smooth flight trajectories while dealing with unexpected dead-ends, avoiding obstacles and taking into consideration the maneuvering limitations of the vehicle.

3. The vehicle's dynamics constraints must be taken into account to prevent the computing the non-executable paths. The inverse simulation module used in the system translates the planned flight path to actual commands accurately enough for the SLAM to cope with the execution errors

4. The proposed methods were tested over different environment. The shown results illustrate the potential of the algorithms and the viability of the combination of these modules for indoor navigation of RW MAVs .

REFERENCES

[1] H. Durrant-Whyte and T. Bailey. Simultaneous Localisation and Mapping (SLAM): Part I. The Essential Algorithms. *Robotics and Automation Magazine*, 13, 2006.

[2] S. Shen, N. Michael and V. Kumar. Autonomous Multi-Floor Indoor Navigation with a Computationally Contrained MAV. In *IEEE Int. Conference on Robotics and Automation*, pages 20–25, Shangai, China, May 2011.

[3] S. Grzonka, G. Grisetti and W. Burgard. Towards a Navigation System for Autonomous Indoor Flying. In *IEEE Int.*

Conference on Robotics and Automation, pages 2878–2883, Kobe, Japan, May 2009.

[4] R. He, S. Prentice and N. Roy. Planning in information space for a quadrotor helicopter in a GPS-denied environment. In *IEEE Int. Conference on Robotics and Automation*, pages 1814–1820, Pasadena, California, USA, May 2008.

[5] C. Friedman, I. Chopra, S. Potyagaylo, O.Rand and Y. Kanza. Towards Model-Free SLAM Using a Single Laser Range Scanner for Helicopter MAV. In *AIAA Guidance, Navigation, and Control Conference*, Portland, USA, August 2011.

[6] S. Thrun. Learning occupancy grid maps with forward sensor models. *Autonomous robots*, 15(2):111–127, 2003.

[7] Khatib O. "Real-time obstacle avoidance for manipulators and mobile robots". *International Journal of Robotics Research*, 5(1), 1986.

[8] D. G. Thomson and R. Bradley. Inverse simulation as a tool for flight dynamics research – principles and application. *Progress in Aerospace Sciences*, 42:174–210, 2006.

[9] S. Thrun, W. Burgard and D. Fox. *Probabilistic Robotics*. The MIT Press, 2005.

[10] D. Hahnel, W. Burgard, D. Fox, and S. Thrun. An Efficient FastSlam Algorithm for Generating Maps of Large-Scale Cyclic Environments from Raw Laser Range Measurements. In *IEEE/RSJ International Conference on Intelligent Robots and Systems*, Las Vegas, NV, USA, October 2003.

[11] A. Diosi and L. Kleeman. Laser Scan Matching in Polar Coordinates with Application to SLAM. In *The IEEE/RSJ International Conference on Intelligent Robots and Systems*, 2005.

[12] A. E. Bryson and Y. C. Ho. *Applied Optimal Control*. Prentice-Hall, Hemisphere, New York, 1975.

[13] D. P. Bertsekas. *Dynamic Programming and Optimal Control*, volume 1-2. Belmont, Mass.: Athena Scientific, 2005-2007.

[14] E. Frazzoli, M. A. Dahleh and E. Feron. Real-time Motion Planning for Agile Autonomous Vehicles. *J. of Guidance, Control, and Dynamics*, 25(1):116–129, 2002.

[15] V. Shaferman and T. Shima. Unmanned Aerial Vehicles Cooperative Tracking of Moving Ground Target in Urban Environment. *J. of Guidance, Control and Dynamics*, 31(5):1360–1370, 2008.

[16] D. G. Thomson and R. Bradley. Development and Verification of an Algorithm for Helicopter Inverse Simulations. *Vertica*, 14(2):185–200, 1990.

[17] R. A. Hess and C. Gao. A Generalized Algorithm for Inverse Simulation Applied to Helicopter Maneuvering Flight. *J. of the American Helicopter Society*, 38(4):3–15, 1993.

[18] G. D. Padfield. *Helicopter Flight Dynamics: The Theory and Application of Flying Qualities and Simulation Modelling*. Oxford: Blackwell, 2007.

[19] ADS-33D-PRF. Aeronautical Design Standard Performance Specification Handling Qualities Requirements for Military Rotorcraft. Technical report, U.S. Army Aviation and Troop Command, 1996.

[20] Hokuyo. UTM-30LX. Technical report, http://www.hokuyo-aut.jp, 2009.

[21] Blade, Horizon Hobby, Inc. http://www.bladehelis.com/.

[22] O. Rand and S.M. Barkai. Numerical Evaluation of the Equations of Motion of Helicopter Blades and Symbolic Exactness. *J. of the American Helicopter Society*, 40(1):59–71, 1995.

[23] Review of RAPID. *Vertiflite*, 42(4), 1996.

[24] O. Rand. Technology Display and Exhibition of the American Helicopter Society 56th Annual Forum, May 2000.

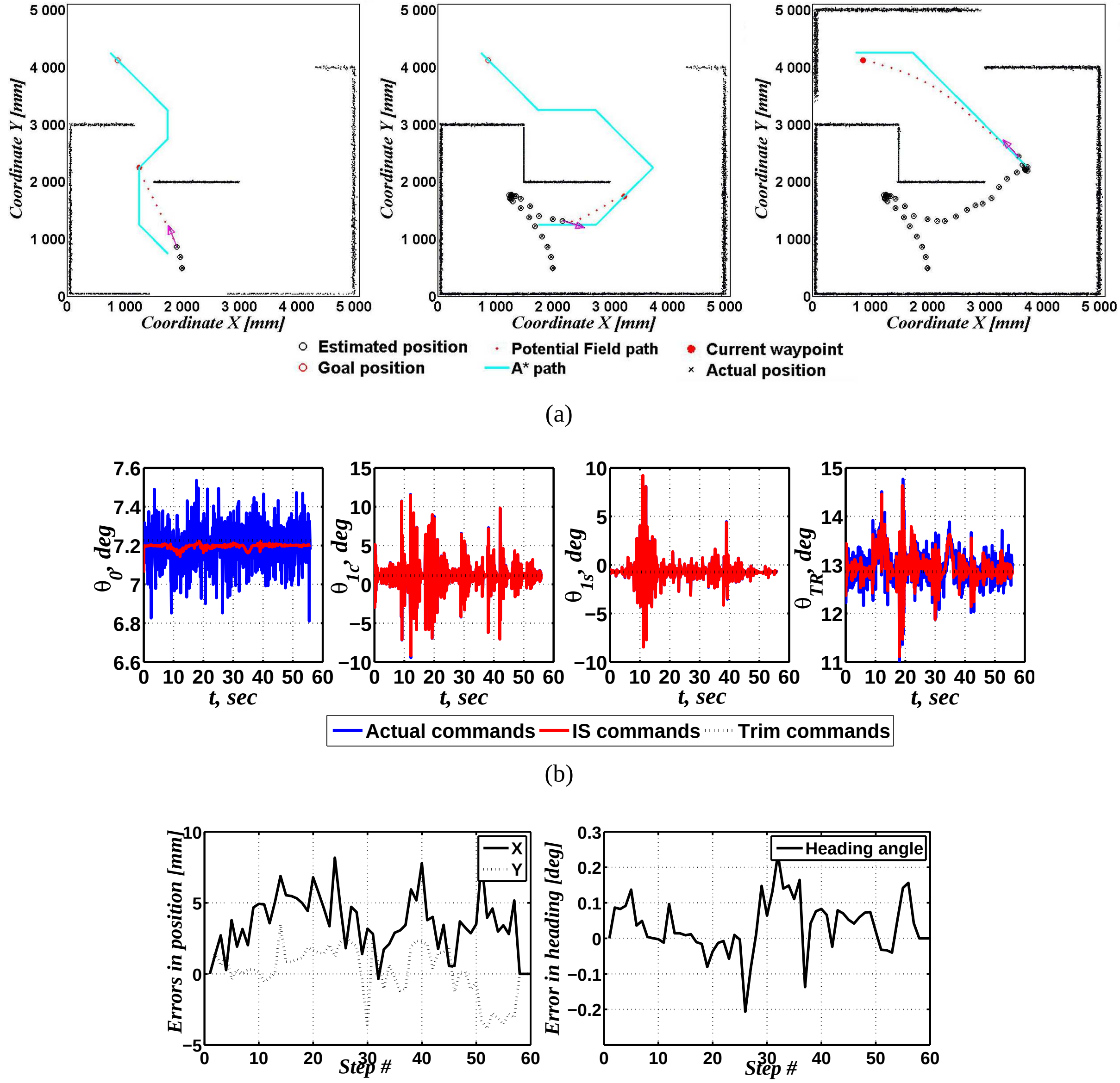

(a)

(b)

(c)

Fig. 7. Flying through an environment whose map is unknown: (a) Left: Initial planned trajectory; Middle: An abrupt heading change due to a dead-end recognition; Right: The final trajectory. (b) The tail rotor collective pitch command and heading angle of the MAV. (c) The differences (errors) between estimated and actual position and orientation of the MAV.